IEEE Photonics Journal
An IEEE Photonics Society Publication

Open Access

Chirp-Compensated DBR Lasers for TWDM-PON Applications

Volume 7, Number 1, February 2015

Hang Zhao
Sheng Hu
Jialin Zhao
Yao Zhu
Yonglin Yu, Member, IEEE
Liam P. Barry, Senior Member, IEEE

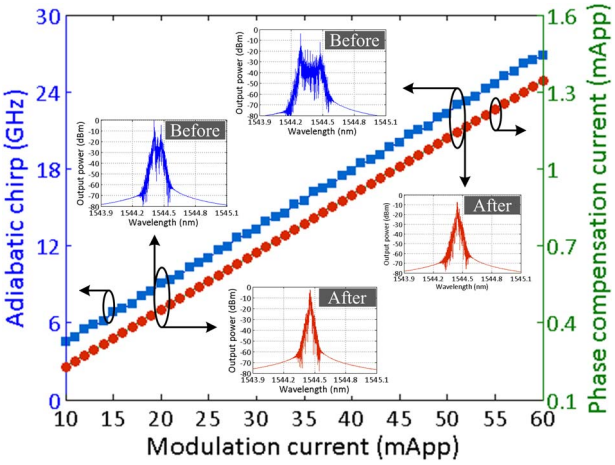

DOI: 10.1109/JPHOT.2015.2392377
1943-0655 © 2015 IEEE

Chirp-Compensated DBR Lasers for TWDM-PON Applications

Hang Zhao,[1] Sheng Hu,[1] Jialin Zhao,[1] Yao Zhu,[1] Yonglin Yu,[1] *Member, IEEE*, and Liam P. Barry,[2] *Senior Member, IEEE*

[1]Wuhan National Laboratory for Optoelectronics, Huazhong University of Science and Technology, Wuhan 430074, China
[2]The Rince Institute, Dublin City University, Dublin 9, Ireland

DOI: 10.1109/JPHOT.2015.2392377
1943-0655 © 2015 IEEE. Translations and content mining are permitted for academic research only. Personal use is also permitted, but republication/redistribution requires IEEE permission. See http://www.ieee.org/publications_standards/publications/rights/index.html for more information.

Manuscript received November 27, 2014; revised January 6, 2015; accepted January 9, 2015. Date of publication February 2, 2015; date of current version February 11, 2015. This work was supported in part by the National High Technology Developing Program of China under Grant 2013AA014503, by the National Natural Science Foundation of China under Grant 11174097, and by the International S&T Cooperation Program of China under Grant 1016. Corresponding author: Y. Yu (e-mail: yonglinyu@mail.hust.edu.cn).

Abstract: We propose a novel chirp compensation scheme for directly modulated three-section distributed Bragg reflector (3s-DBR) lasers in applications of the time- and wavelength-division multiplexed passive optical network systems. The frequency chirp of 3s-DBR lasers induced by direct modulation is investigated through extensive numerical simulations based on the time-domain travel-wave model. To overcome the signal distortions resulting from the frequency chirp due to direct modulation, we extend on our novel idea of frequency chirp compensation technology with inherent characteristics of DBR-type tunable lasers. Q factors and extinction ratio for different system transmission lengths are analyzed and compared. Large dispersion tolerance of the system is achieved by using the chirp compensation scheme.

Index Terms: Three-section DBR laser, chirp compensation, TWDM-PON, long reach.

1. Introduction

Many passive optical network (PON) technologies have been proposed to meet the ever-increasing bandwidth demand for the next generation of fiber access networks [1]–[4]. The time and wavelength division multiplexed PON (TWDM-PON) has attracted the majority support from global vendors and was selected as a primary solution to NG-PON2 [5]. Then, the world's first full-system 40 Gb/s TWDM-PON prototype was demonstrated [6], and four pairs of wavelengths were used in their prototype, and each optical network unit (ONU) can provide peak rates up to 10 Gb/s and 2.5 Gb/s in downstream and upstream, respectively.

The only significantly new components in TWDM-PON are the tunable receivers and tunable transmitters employed at the ONU when compared with G-PON and XG-PON [6]. The ONU transmitter should be capable of being tuned to any of the upstream wavelengths. In this sense, tunable lasers are attractive. A number of novel widely tunable laser sources have been developed during the past two decades [7]–[9]. However, the complicated currents control and fabrication which requires electron beam or high resolution lithography for defining the gratings significantly increase the chip cost. Three section distributed Bragg reflector (3s-DBR) lasers are a good compromise. They generally provide more power than sampled-grating DBR

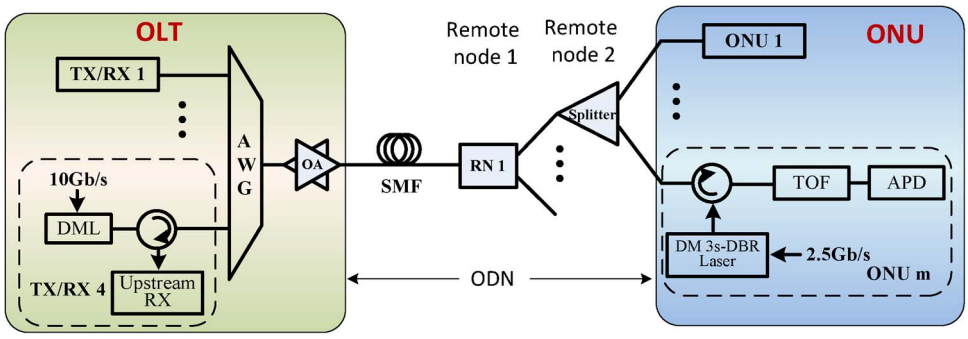

Fig. 1. Architecture of an asymmetric TWDM-PON system.

(SG-DBR) lasers, super-structure-grating DBR(SSG-DBR) lasers, and digital supermode DBR (DS-DBR) lasers, a wider tuning range than the thermally tuned DFB laser, and importantly, they only require a simple technological process [10], [11]. In addition, 3s-DBR lasers operating at 2.5 Gb/s were shown to be a good candidate for ONU transmitters in a hybrid 40 Gb/s G-PON system [12].

Another important consideration for access networks is the modulation technique employed at the ONU's. As compared to external modulation (EM) schemes such as electro-absorption modulator (EAM) or Mach-Zehnder modulator (MZM), direct modulation is one of the most simple and cost-efficient techniques to modulate lightwaves in cost-sensitive metro and access optical links. However, for directly modulated lasers (DMLs), the carrier density is modulated via drive current and this carrier change can give rise to an inherent and highly component-specific frequency chirp. In DML based PON systems, this positive frequency chirp results in spectrum broaden that severely limits the maximum achievable system transmission performance due to fiber dispersion, especially for the long reach applications ($>$ 60 km) [13]. One way to overcome this issue is to use special fibers with a negative dispersion characteristic [14], however, it is not practical to upgrade and change the installed base of metro fiber links. Another approach is to use the chirp-managed laser (CML) which employs a suitable optical filter to control the phase between the adjacent bits [15], but it requires an additional wavelength specific module. Also, electronic pre-compensation for a 10.7 Gb/s system under direction modulation has been investigated in [16], but this required additional signal processing after the receiver.

In this work, we investigate 3s-DBR laser characteristics under direct modulation and demonstrate a novel chirp compensation scheme which can be used in the ONUs for the long reach TWDM-PON systems. An example of an asymmetric 40 Gb/s TWDM-PON system equipped with 3s-DBR lasers is shown in Fig. 1. Four transmitters and receivers (TXs/RXs) units are used in the OLT, and each transmitter is directly modulated by 10 Gb/s signals. The ONUs are equipped with tunable transmitters and receivers, where 10 nm tuning range 3s-DBR lasers with 2.5 Gb/s direct modulation are used so that any of the four upstream wavelengths can be reached. To overcome the signal distortions resulting from the frequency chirp due to direct modulation, we extend on our novel idea of the frequency chirp compensation technology with inherent characteristics of DBR type tunable lasers [17]. For achieving the optimum compensation, the chirp characteristics of 3s-DBR lasers induced by direct modulation are investigated with extensive numerical simulations. Q-factors and ER for different system transmission lengths are analyzed and compared. Large dispersion tolerance of the system is demonstrated by using the chirp compensation. Results implicate that the proposed scheme might have promising applications in long reach TWDM-PON systems.

2. Frequency Chirp in Direct Modulation of 3s-DBR Lasers

The structure of a 3s-DBR laser is depicted in Fig. 2(a). The simulated 3-D wavelength tuning map and superimposed tuning spectra of the 3s-DBR laser are shown in Fig. 2(b) and (c) respectively. Our simulations are based on the time-domain travelling-wave (TDTW) model [18].

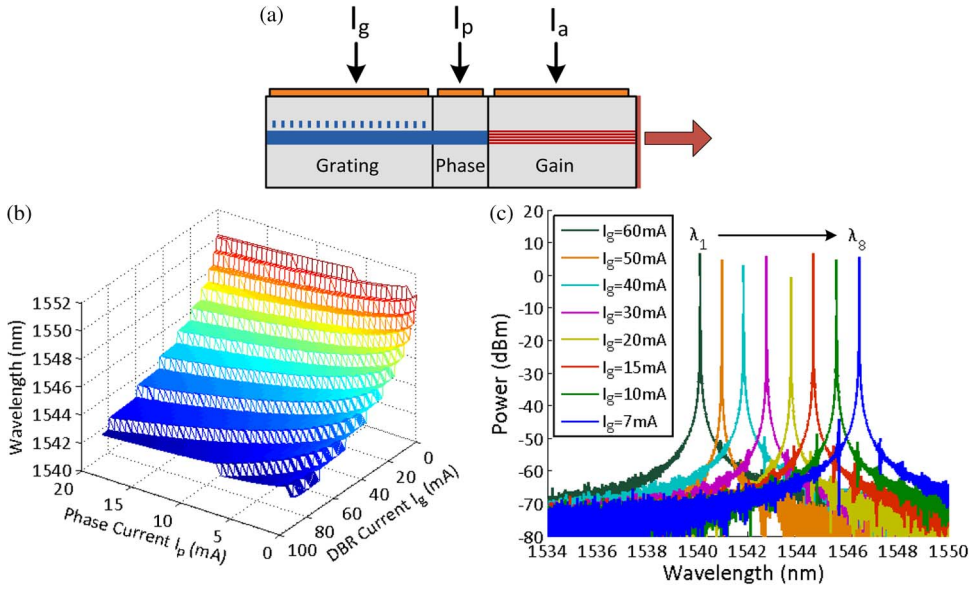

Fig. 2. Structure of 3s-DBR laser (a) and its static tuning characteristics. (b) Three-dimensional surface of lasing wavelength. (c) Superimposed tuning spectra of eight ITU wavelength channels.

First, we can obtain the output optical field in time domain by solving the time-dependent coupled wave equations. Then, the lasing wavelength can be confirmed by transforming the time-dependent field using a fast Fourier transform. As a result, static characteristics including the tuning map can be obtained by varying both the phase current and grating current respectively. A tuning range from 1539 to 1549 nm with 100 GHz mode interval has been achieved and each of the map steps represents a lasing mode when a longitudinal mode of the cavity coincides with the Bragg reflection peak. Fig. 2(c) gives the superimposed lasing spectra for eight ITU wavelength channels in the C-band. The structure parameters used in our simulation are listed in Table 1, similar to [19].

The frequency chirp $\Delta\nu(t)$ of directly modulated 3s-DBR lasers can be expressed as

$$\Delta\nu(t) = \frac{\alpha_H}{4\pi}\left\{\frac{1}{P(t)}\frac{dP(t)}{dt} + \kappa P(t)\right\} \tag{1}$$

where α_H represents the linewidth enhancement factor, and $\kappa = 2\Gamma_1\varepsilon/\eta h\nu V$ is the adiabatic chirp coefficient, which can be calculated with the values listed in Table 1.

We simulate the chirp characteristics combined the chirp expression (1) with the developed TDTW model. The input signals used in the simulation is a Super-Gaussian-shaped pseudorandom binary sequence (PRBS) with a length of $2^7 - 1$ can be generated by MATLAB. Simulated results are shown in Fig. 3, where the active, phase and grating section current is biased at 60, 5.5, and 15 mA, respectively. In this case, the laser operates at 1544.5 nm (194.1 THz). The modulation amplitude of the driving current is 30 mA and the signal is directly modulated at 2.5 Gb/s in NRZ modulation format. The rising and falling time of the modulation signal are approximately 150 ps. Fig. 3(a) shows simulated chirp under direct modulation. The green plot presents the transient chirp due to the first term in (1), which is a structure-independent chirp. While, the blue plot in Fig. 3(a) presents the adiabatic chirp corresponding the second term in (1), which is a structure-dependent chirp. Fig. 3(b) shows the output power and total frequency chirp of 3s-DBR lasers. A large frequency chirp of 12 GHz occurs and the transient chirp has been completely "masked" by the adiabatic term.

To observed distortions on the signal due to the frequency chirp resulting from the directly modulated 3s-DBR lasers, eye diagrams, Q factor and ER are simulated and analyzed. First, a PRBS bit sequence is applied on the laser, then the modulated optical field from the laser output

TABLE 1

Empirical values used in the simulation

Parameters	Symbol	Value
Active section		
Length	l_1	250 μm
Width	w_1	1.2 μm
Thickness	d_1	0.18 μm
Refractive index	n_{01}	3.4
Group Refractive index	n_{ga}	3.56
Internal absorption	α_{01}	$2100m^{-1}$
Nonradiative recombination coefficient	A	$1\times10^{8}/s$
Radiative recombination coefficient	B	$8\times10^{-17}m^3/s$
Auger recombination coefficient	C_1	$7.5\times10^{-41}m^6/s$
Gain coefficient	g_N	$2\times10^{-20}m^2$
Index derivative with respect to carrier density	dn/dN	$-1.5\times10^{-26}m^3$
Linewidth enhancement factor	α_H	6
Gain compression factor	ε	$4.3\times10^{-23}m^3$
Confinement factor	Γ_1	0.3
Passive section		
Length of phase section	l_2	120 μm
Length of DBR section	l_3	300 μm
Width of waveguide	w_p	1.2 μm
Thickness of waveguide	d_p	0.3 μm
Group Refractive index	n_{gp}	3.4
Confinement factor	Γ_p	0.32
Auger recombination coefficient	C_2	$4\times10^{-41}m^6/s$
Normalized coupling coefficient	ζl_3	3

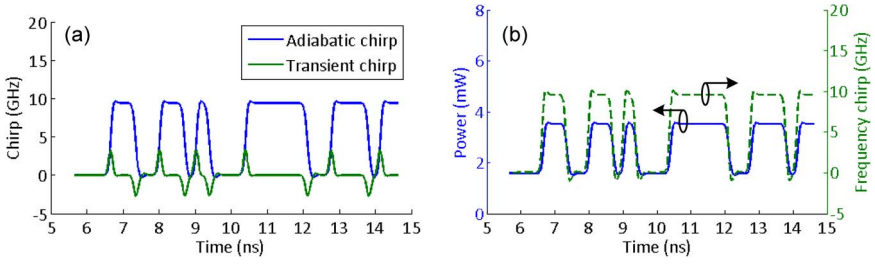

Fig. 3. Simulated directly modulated 3s-DBR laser driven by 2.5 Gb/s NRZ PRBS signals. (a) Adiabatic chirp and transient chirp. (b) Output power and total frequency chirp.

can be extracted in time domain. This optical field contains the chirp information induced by the direct modulation. So after fiber transmission, the distorted signals caused by fiber dispersion can be obtained. Then eye diagrams, Q factor and ER can be acquired and calculated. The empirical values for the laser are listed in Table 1. The fiber used in our simulation is SMF-28 with the dispersion coefficient of 18 ps/nm/km and the attenuation coefficient of 0.2 dB/km.

Fig. 4 shows simulated results of received eye diagrams, for different cases of 3s-DBR lasers with frequency chirp, i.e., transmission over 40 km, 80 km, and 120 km of SMF-28 fiber respectively. It is obvious from the simulations that the effects on the received bit pattern of the interplay of the chirp with the dispersion result in the formation of an intense peak either in isolated 1 s or in the first “1” of a series of 1 s and an increased trailing tail of the pulses.

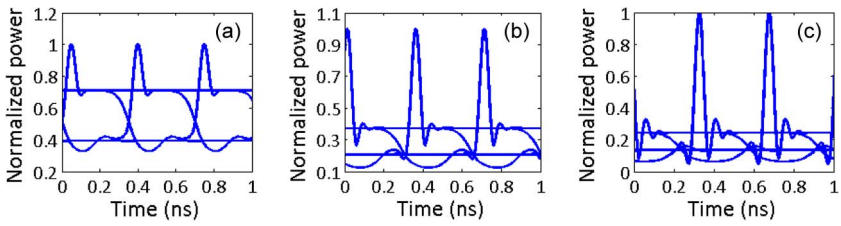

Fig. 4. Simulated eye diagrams without the chirp compensation for transmission over (a) 40-km of SMF-28 fiber, (b) 80-km of SMF-28 fiber, and (c) 120-km of SMF-28 fiber, where the active section is biased at 60 mA, and modulation current is kept at 30 mA.

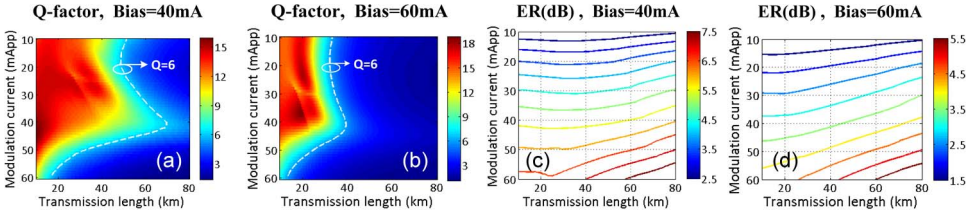

Fig. 5. Calculated Q-factor [(a) and (b)] and extinction ratio (ER) [(c) and (d)] as functions of transmission length and modulation current before the chirp compensation at 40 mA and 60 mA.

Fig. 5 shows the calculated Q-factors [(a) and (b)] and ER [(c) and (d)] as functions of transmission length and modulation current of the directly modulated 3s-DBR laser, for two different biases (40 mA and 60 mA). Here, the quality factor (Q) and extinction ratio (ER) are defined

$$Q = \frac{P_{1\,\mathrm{avg}} - P_{0\,\mathrm{avg}}}{\sigma_1 + \sigma_0}, \quad \mathrm{ER} = 10\log_{10}\left(\frac{P_{1\,\mathrm{avg}}}{P_{0\,\mathrm{avg}}}\right) \tag{2}$$

where $P_{1,0\,\mathrm{avg}}$ and $\sigma_{1,0}$ are the average power and standard deviation for "1" and "0" bits of the fluctuating optical power that reach the receiver. The white dash lines in Fig. 5(a) and (b) correspond to $\mathrm{Q} = 6$ $(\mathrm{BER} = 10^{-9})$. The different color lines in Fig. 5(c) and (d) represent contour lines of ER. The low bias current generates a large relaxation oscillation, thus increasing the transient chirp and impairing system performances, while the high bias current reduces the ER and causes degradation of system performance. At the same time, the small modulation current also reduces the ER while large modulation current can improve the ER but causes the adiabatic chirp to increase. Thus, there is a tradeoff between the bias current and the modulation current, and both of them should be optimized to some extent for achieving good system performance. For example, in Fig. 5(a), when the modulation current is 20 mApp, the maximum transmission length is 50 km, however the corresponding ER is only about 3.5 dB, which can be observed from Fig. 5(c). ER can be improved to 6 dB by increasing the modulation current to 50 mApp, however, the maximum transmission distance will decrease to 32 km.

3. Chirp Compensation Scheme and Performance Improvements

A novel frequency chirp compensation scheme for directly modulated SG-DBR tunable lasers was proposed and demonstrated with experiments in our previous work [17]. By using the compensation technique, the frequency chirp was significantly reduced. The chirp profile and spectra with and without compensation were measured. However, only a four bit patterned sequence of 1100 was used and transmission experiments were not carried out due to some limitations.

Here, we extend this novel idea from the inherent advantage of the DBR type tunable lasers, to overcome the signal distortions resulting from the frequency chirp due to directly modulated 3s-DBR lasers for the proposed asymmetric TWDM-PON application as shown in Fig. 1. The

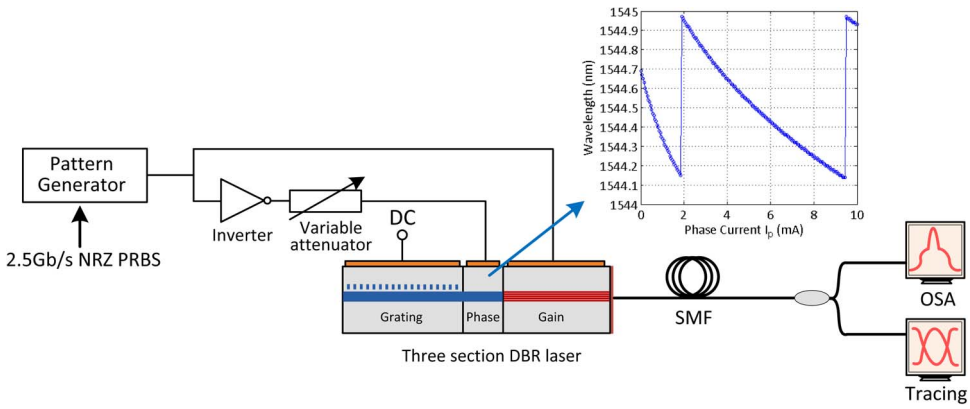

Fig. 6. Schematic setup for the proposed chirp compensation method.

chirp compensation is indeed based on the fact that the frequency chirp exhibited by the active and phase sections have opposing signs when the laser is directly modulated by an identical bit sequence. However, the compensation current into the phase section must be optimized to achieve accurate frequency shifts. For this purpose, the chirp characteristics of a 3s-DBR laser under direct modulation are analyzed with extensive numerical simulations. We also calculated Q-factors and ER at different bias and modulation current for different transmission lengths to estimate the system performances.

The proposed chirp compensation scheme is described in Fig. 6. A string of NRZ data is split into two paths. One is used to drive the active section and the other is connected to the phase section passing through an inverter and variable attenuator. The inset of Fig. 6 shows that the characteristic of frequency verse the phase section current, which can be utilized to reduce the inherent chirp associated with direct modulation on the active section if the frequency variation has a sign that is opposite of the chirp. The total frequency deviation after the proposed chirp compensation can be expressed as

$$\Delta\nu = \frac{\alpha_H}{4\pi}\left\{\frac{1}{P(t)}\frac{dP(t)}{dt} + \kappa P(t)\right\} - \frac{\nu\frac{dn}{dN}\Delta N_p L_p}{n_{ga}L_a + n_{gp}L_p} \tag{3}$$

where the first term is the frequency chirp and the second term is the frequency deviation caused by passive section, respectively. dn/dN is the index derivative with respect to carrier density, n_{gi} $(i = a, p)$ is the group refractive index. The values of parameters used in (3) can be found in Table 1. Clearly, from (3), the best chirp compensation can be achieved by optimization of currents on active section and passive section.

In the case of modulated rates at 2.5 Gb/s and the large value of nonlinear gain suppression coefficient, the transient chirp will be compressed since it can be easily masked by adiabatic chirp. As a result, adiabatic chirp compensation becomes the real problem that needs to be resolved. We first characterize the relationship between adiabatic chirp and modulation current, and then determine the phase current required for compensation. As shown in Fig. 7 we can see that there is an approximate linear relationship between adiabatic chirp and modulation current depicted by blue squares, while the phase compensation current required for each level of modulation current is depicted by red dots. Four insets in Fig. 7 shows the spectra before and after the chirp compensation for two different modulation currents (20 mApp and 50 mApp). When the modulation current is 20 mApp, the adiabatic chirp induced spectrum broadening is 10 GHz, and the spectrum will be broadened up to 25 GHz if the modulation current increases to 50 mA. The spectra are clearly compressed after adding the phase compensation currents. The narrowing in the spectrum mirrors the reduction in chirp as implied in (3).

The received eye diagrams with chirp compensation when 3s-DBR laser is driven with the 2.5 Gb/s PRBS NRZ signals, for transmission distances of 40 km, 80 km, and 120 km are

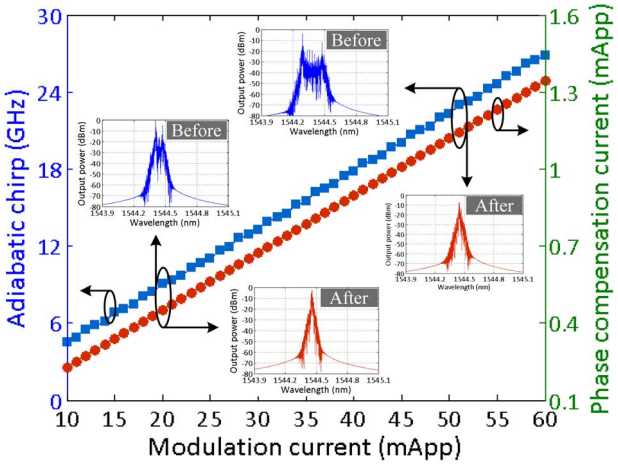

Fig. 7. Adiabatic chirp and corresponding phase compensation current at different modulation current.

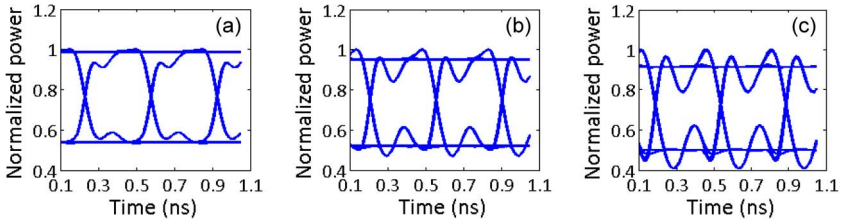

Fig. 8. Simulated eye diagrams for the chirp compensated signals at 2.5 Gb/s for transmission over (a) 40-km, (b) 80-km, and (c) 120-km of SMF-28 fiber. The bias and modulation current are kept at 60 mA and 30 mApp, respectively.

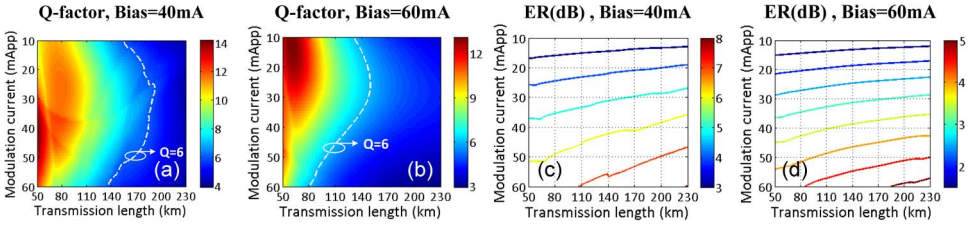

Fig. 9. Calculated Q-factor [(a) and (b)] and extinction ratio (ER) [(c) and (d)] at different bias as functions of transmission length and modulation current after the chirp compensation.

shown in Fig. 8. Compared with Fig. 4, we can see that the quality of eye diagrams were greatly improved and that signals can be transmitted farther with less deterioration.

To reaffirm the chirp compensation technique, the Q-factor [(a) and (b)] and ER [(c) and (d)] are calculated at different bias and modulation currents, for different transmission lengths, as shown in Fig. 9. One can clearly find that with chirp compensation the Q-factor does not decrease dramatically with the increase of transmission distance, compared to Fig. 5. ER of 7 dB can be obtained by applying 55 mApp modulation current on the laser and meanwhile more than 120 km transmission distance can be reached when the laser is biased at 40 mA. The BER curves of 2.5 Gb/s signal with three different modulation amplitudes before and after chirp compensation are shown in Fig. 10. It is shown that after chirp compensation, the transmission distance is significantly extended. In addition, high modulation current amplitude can be used to get large ER without fear of the dispersion penalty.

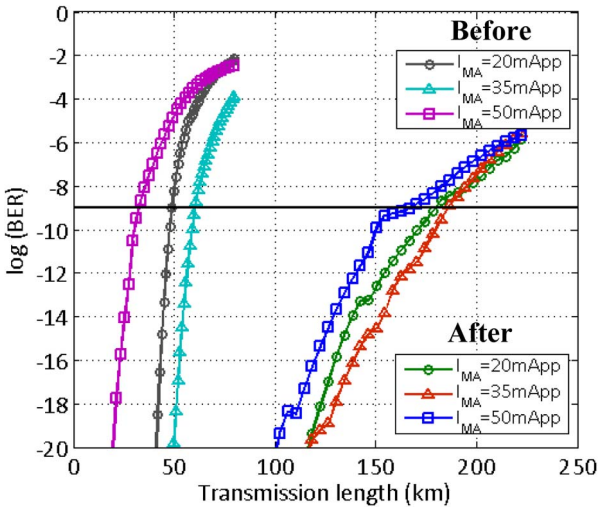

Fig. 10. BER curves of 2.5 Gb/s signal with different modulation amplitude before and after chirp compensation when the active section is biased at 40 mA.

We are currently working on some related practical issues, such as the device fabrication, the drive electronics and packaging, and planning to carry out experimental demonstrations in the next phase. The use of 3s-DBR lasers at 10 Gb/s and without the temperature controller are expected to boost the transmission rate and reduce the cost of the ONU's for WDM-PON applications. We would like to investigate possibilities of extension of our compensation method to these cases in the next phase as well.

4. Conclusion

We propose a novel chirp compensation scheme for directly modulated 3s-DBR lasers in the applications of the TWDM-PON systems. Frequency chirp of the directly modulated 3s-DBR lasers at 2.5 Gb/s was investigated based on time-domain travel-wave (TDTW) model. Results show that the spectrum could be broadened up to 25 GHz due to the adiabatic chirp and thus system performances, such as Eye diagrams, Q factor and ER degrade dramatically with the increase of transmission distance. By using the chirp compensation technique, the spectrum of the laser is greatly compressed, and signals can be transmitted more than 120 km with $Q > 6$ $(\mathrm{BER} < 10^{-9})$ and $\mathrm{ER} > 6$ dB. In this sense, the proposed scheme might provide a cost-effective solution for long reach asymmetric 40 Gb/s TWDM-PON systems.

References

[1] "10-Gigabit-capable passive optical networks (XG-PON): General requirements," ITU-T Recommendation G.987.1 Int. Telecommun. Union, Geneva, Switzerland, Jan. 2010.
[2] H. K. Lee, H. S. Cho, J. Y. Kim, and C. H. Lee, "A WDM-PON with an 80 Gb/s capacity based on wavelength-locked Fabry–Perot laser diode," *Opt. Exp.*, vol. 18, no. 17, pp. 18 077–18 085, Aug. 2010.
[3] K. Grobe and J. P. Elbers, "PON in adolescence: From TDMA to WDM-PON," *IEEE Commun. Mag.*, vol. 46, no. 1, pp. 26–34, Jan. 2008.
[4] W. Wei, C. Wang, and T. Wang, "Optical orthogonal frequency division multiple access networking for the future Internet," *IEEE/OSA J. Opt. Commun. Netw.*, vol. 1, no. 2, pp. 236–246, Jul. 2009.
[5] F. Effenberger, "XG-PON1 versus NG-PON2: Which one will win?" in *Proc. Eur. Conf. Exhib. Opt. Commun.*, 2012, p. Tu.4.B.1.
[6] Y. Luo *et al.*, "Time and wavelength division multiplexed passive optical network (TWDM-PON) for next generation PON stage 2 (NG-PON2)," *J. Lightw. Technol.*, vol. 31, no. 6, pp. 587–593, Feb. 2013.
[7] B. Mason, G. Fish, S. DenBaars, and L. A. Coldren, "Widely tunable sampled-grating DBR laser with integrated electroabsorption modulator," *IEEE Photon. Technol. Lett.*, vol. 11, no. 6, pp. 638–640, Jun. 1999.
[8] H. Ishii *et al.*, "Quasicontinuous wavelength tuning in super-structure-grating (SSG) DBR lasers," *IEEE J. Quantum Electron.*, vol. 32, no. 3, pp. 433–441, Mar. 1996.

[9] A. J. Ward *et al.*, "Widely tunable DS-DBR laser with monolithically integrated SOA: Design and performance," *IEEE J. Sel. Topics Quantum Electron.*, vol. 11, no. 1, pp. 149–156, Jan./Feb. 2005.
[10] T. L. Koch, U. Koren, R. P. Gnall, C. A. Burrus, and B. I. Miller, "Continuously tunable 1.5 um multiple quantum well GaInAs/GaInAsP distributed Bragg reflector laser," *Electron. Lett.*, vol. 24, no. 23, pp. 1431–1433, Nov. 1988.
[11] S. H. Oh *et al.*, "Fabrication and lasing characteristics of tunable integrated-twin-guide distributed Bragg reflector laser diode and butt coupled distributed Bragg reflector laser diode," *J. Korean Phys. Soc.*, vol. 42, pp. S591–S596, Feb. 2003.
[12] X. Yan *et al.*, "Tunable laser for 40GPON ONU transmitter," in *Proc. OFC/NFOEC*, 2012.
[13] R. P. Davey *et al.*, "Long-reach passive optical networks," *J. Lightw. Technol.*, vol. 27, no. 3, pp. 273–291, Feb. 2009.
[14] I. Tomkos *et al.*, "Transmission of 1550 nm 10 Gb/s directly modulated signal over 100 km of negative dispersion fiber without any dispersion compensation," in *Proc. OFC*, 2000, p. TuU6.
[15] J. Yu *et al.*, "Applications of 40-Gb/s chirp-managed laser in access and metro networks," *J. Lightw. Technol.*, vol. 27, no. 3, pp. 253–265, Feb. 2009.
[16] A. S. Karar, J. C. Cartledge, J. Harley, and K. Roberts, "Electronic pre-compensation for a 10.7-Gb/s system employing a directly modulated laser," *J. Lightw. Technol.*, vol. 29, no. 13, pp. 2069–2076, Jul. 2011.
[17] R. Maher *et al.*, "Novel frequency chirp compensation scheme for directly modulated SG DBR tunable lasers," *IEEE Photon. Technol. Lett.*, vol. 21, no. 5, pp. 340–342, Mar. 2009.
[18] L. M. Zhang, S. F. Yu, M. Nowell, D. D. Marcenac, and J. E. Carroll, "Dynamic analysis of radiation and side mode suppression in second order DFB lasers using time-domain large signal traveling wave model," *IEEE J. Quantum Electron.*, vol. 30, no. 6, pp. 1389–1395, Jun. 1994.
[19] X. Pan, H. Olesen, and B. Tromborg, "A theoretical model of multielectrode DBR lasers," *IEEE J. Quantum Electron.*, vol. 24, no. 12, pp. 2423–2432, Dec. 1988.